Deep–Sea Research II 222 (2025) 105498

Contents lists available at ScienceDirect

Deep-Sea Research Part II

journal homepage: www.elsevier.com/locate/dsr2

On the sensitivity of Optimum Multiparameter Analysis: a California Current System case study

Mercedes Pozo Buil [a,*], Isaac Schroeder [a], Steven J. Bograd [a,b], Michael G. Jacox [a,b,c], Elliott L. Hazen [a,b], Dianne Deauna [d], Emanuele Di Lorenzo [e], Nicole S. Lovenduski [f], Samuel Mogen [f], Ryan R. Rykaczewski [d,g]

[a] Institute of Marine Sciences, University of California-Santa Cruz, Santa Cruz, CA, USA
[b] NOAA Southwest Fisheries Science Center, Monterey, CA, USA
[c] NOAA Physical Sciences Laboratory, Boulder, CO, USA
[d] School of Ocean and Earth Science and Technology, University of Hawai'i at Manoa, Honolulu, HI, USA
[e] Department of Earth, Environmental, and Planetary Sciences, Brown University, Providence, RI, USA
[f] Department of Atmospheric and Oceanic Sciences, Institute of Arctic and Alpine Research, University of Colorado Boulder, Boulder, CO, USA
[g] NOAA Pacific Islands Fisheries Science Center, Honolulu, HI, USA

A R T I C L E I N F O

Handling editor: K Drinkwater

Keywords:
Optimum multiparameter analysis
Water masses
California current system
Eastern boundary upwelling systems
Source water characteristics

A B S T R A C T

Eastern boundary upwelling systems, like the California Current System (CCS), represent a confluence and mixing of water masses whose variability and composition play a key role in modulating their high biological productivity and ecosystem variability. In the southern CCS, the relative contribution (i.e. proportion) and variability of its source water masses was quantified previously using an extended Optimum MultiParameter (eOMP) analysis, which is an inverse modeling technique that solves a set of linear mixing equations using quasi-conservative and non-conservative properties. However, there are several oceanographic decisions implicit in eOMP analysis that can generate uncertainties in the representation of the mixing and proportions of the source waters in a region. Here we quantify the sensitivity of these previous eOMP results in the southern CCS to varying oceanographic assumptions based on the uncertainty of the water mass properties, modified Redfield ratios, and alternate locations of the eastern tropical Pacific source waters. We show that the mean relative contributions of the main CCS source waters are more sensitive to the location of their selected source region (~20–25 %) and the Redfield ratio (~15–20 %) than to the uncertainty in the source water properties (~2–5 %). Understanding the uncertainties of the eOMP assumptions benefits similar studies in other regions, especially in other eastern boundary upwelling systems (EBUS) where water masses characteristics and composition strongly impact the ecosystem.

1. Introduction

Variability in water mass distributions and properties play a key role in modulating regional ecosystem responses to large-scale changes in ocean circulation and climate conditions. For more than a century, scientists have analyzed the subsurface properties of the ocean to better understand the variable distribution of characteristic water masses. Such analyses include classic (and typical) techniques that use two or three characteristic properties: potential temperature and salinity diagrams (θ-S diagram) or the mixing triangle approach, introduced by Helland-Hansen (1916), volumetric θ-S analysis, introduced by Montgomery (1958), temporal diagrams (e.g. θ-S-time), and more quantitative analysis that can use several properties, like the Optimum MultiParameter analysis (OMP, Tomczak, 1981).

Optimum MultiParameter (OMP) analysis objectively determines the relative contribution (i.e. proportion) of the water masses in a region by applying an inverse modeling technique to solve a set of linear mixing equations. In contrast to the classical mixing diagram, which is usually based on θ and S, OMP analysis utilizes additional characteristic properties beyond θ and S, such as nutrients, oxygen, and potential vorticity.

This article is part of a special issue entitled: EBUS published in Deep-Sea Research Part II.

* Corresponding author. 99 Pacific St., Unit 255A, Monterey, CA 93940, USA.
E-mail address: mpozobui@ucsc.edu (M. Pozo Buil).

https://doi.org/10.1016/j.dsr2.2025.105498
Received 26 April 2024; Received in revised form 7 May 2025; Accepted 30 May 2025
Available online 1 June 2025
0967-0645/

OMP analysis was first introduced by Tomczak (1981), and then developed formally with a least squares approach by Mackas et al. (1987). The inclusion of potential vorticity was introduced later in OMP analysis (Tomczak, 1999), although it is less commonly used than the classical tracers **θ**, S, nutrients, and oxygen. OMP analysis has been applied in multiple studies around the world to understand regional mixing and circulation (García-Ibáñez et al., 2018; Jenkins et al., 2015; Tomczak, 1999a,b), model thermohaline circulation in the Indian (You and Tomczak, 1993), Atlantic (Poole and Tomczak, 1999), and Southern (Pardo et al., 2012) Oceans, and to quantify the ventilation of oxygen minimum zones, OMZ (Karstensen and Tomczak, 1997; Llanillo et al., 2013), among others.

For the upwelling system of the California Current System (CCS), Bograd et al. (2019) applied the OMP analysis to quantify the spatio-temporal variability of the water mass contributions to its southern region. In the southern CCS, the upper-ocean waters are characterized by a confluence and mixing of water masses originating in the subarctic, subtropical, and tropical eastern Pacific (Bograd and Lynn, 2003; Lynn and Simpson, 1987): Pacific Subarctic Upper Water (PSUW), Pacific Equatorial Water (PEW), Eastern North Pacific Central Water (ENPCW). These water masses have properties that are clearly expressed along isopycnals (Bograd et al., 2015) and originating in known regions. PSUW is a near-surface water mass characterized by relatively low temperature and salinity with high oxygen and nutrient content and a core potential density of 25.8 kg/m^3. PEW is characterized by relatively elevated temperature and salinity, reduced oxygen, high nutrient content, and a core potential density of 26.5 kg/m^3. ENPCW is evident as relatively warm and salty near-surface water with low nutrient and oxygen content and a core potential density of 25.4 kg/m^3 (Bograd et al., 2019). In the southern CCS, the climatological spatial distribution of these water masses reflects the main circulation (Fig. 1). Higher percentages of PSUW (~60 %) are mainly located in the surface offshore regions, reflecting the influence of the California Current, which transports the PSUW from the north. The subsurface inshore of the southern CCS is characterized by higher percentages of PEW (~50 %) with strong seasonality, reflecting the core of the California Undercurrent (CU) that advects PEW from Baja California (Gómez-Valdivia et al., 2017; Thomson and Krassovski, 2010) into the region. The highest percentages of ENPCW (~30 %) are limited to the upper-waters offshore of the southern CCS, reflecting the intrusion of the North Pacific Subtropical Gyre into the region (Bograd et al., 2019).

Variability in the relative contributions of water masses is a consequence of large-scale climate variability. In the southern CCS, Bograd et al. (2019) showed that the primary contributions of the source waters exhibit strong interannual variability in both their content and depth distribution. In spring and fall, the subsurface component of the Mexican Coastal Current strengthens and bifurcates into two branches: one continues along the coast of mainland Mexico, while the other crosses the Gulf of California and joins the CU, providing an external source of momentum that drives its semiannual variability (Gómez-Valdivia et al., 2015). During El Niño years, the thermocline is characterized by more PSUW content offshore, and lower content inshore during La Niña years. In contrast, the deeper thermocline is characterized with more PEW content inshore during El Niño than during La Niña years, although there is a higher content of PEW in the upper thermocline during La Niña years. The higher contribution of PEW during El Niño periods reflects the stronger advection of the CU from the south (e.g. Gómez-Valdivia et al., 2017). The sensitivity of changing water-mass contributions in the CCS to the El Niño–Southern Oscillation (ENSO) demonstrates how changes in climate and ocean conditions can drive variability in

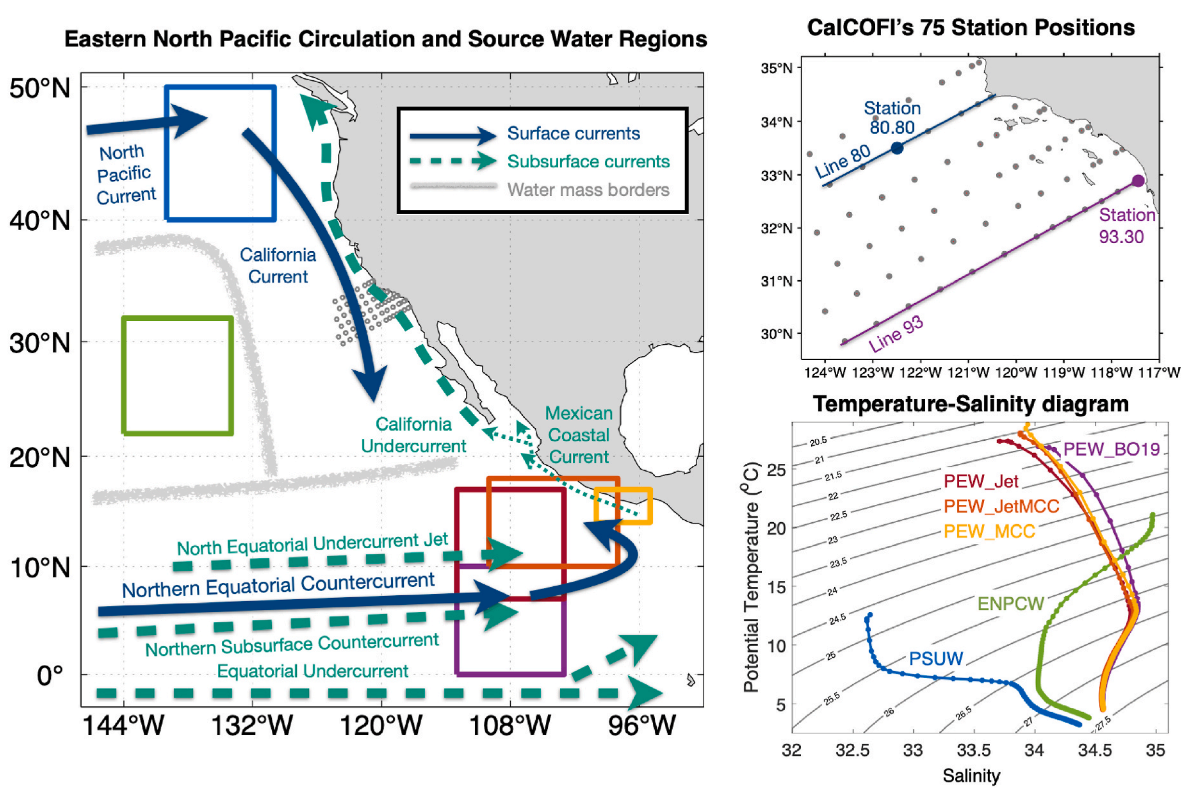

Fig. 1. (left) Schematic of eastern North Pacific showing the source water regions for Pacific Subarctic Upper Water (PSUW; blue box), Eastern North Pacific Central Water (ENPCW; green box), and Pacific Equatorial Water (PEW$_{BO19}$; purple box), the proposed PEW source regions for the sensitivity experiments: Jet (red box), JetMCC (orange box), and MCC (yellow box). The dominant surface and subsurface currents are also shown. (top right) Nominal CalCOFI grid showing stations. Lines 80 and 93, and stations 80.80 and 93.30 are labeled. (bottom right) Temperature-salinity diagram for PSUW (blue), ENPCW (green), PEW$_{BO19}$ (purple), PEW$_{Jet}$(red), PEW$_{JetMCC}$(orange), PEW$_{MCC}$(yellow). Data obtained from the World Ocean Database (WOD18) for the period 1984–2017. (For interpretation of the references to colour in this figure legend, the reader is referred to the Web version of this article.)

hydrographic and biogeochemical conditions at a regional scale. More details about the spatial-temporal variability of these water masses can be found in Bograd et al. (2019, BO19 hereinafter).

Changes in water mass contributions are a key mechanism by which climate variability is translated into ecosystem impacts. In the southern CCS, observed trends in deoxygenation (e.g. Bograd et al., 2015) has been attributed mostly to changes in PEW contribution (Evans et al., 2020). Positive trends in the contribution of PEW both inshore and off the shelf have been associated with an increase of warm-water (i.e. tropicalization) ichthyoplankton of important commercial and forage fish species (e.g. McClatchie et al., 2016, 2018). On the other hand, greater contribution of PSUW has been associated with higher recruitment and better habitat quality (higher growth and survival) for rockfishes in the southern CCS (Fennie et al., 2023; Schroeder et al., 2019). Because water mass contributions and their properties play an important role regulating ecosystem structure and function in the CCS, obtaining accurate representation of these water masses and their variability is key for developing indicators of ecosystem functioning.

OMP analysis determines the relative proportions of the source waters in a region and is a useful tool to translate large-scale dynamics (and subsequent changes in physical and BGC properties) into regional ecosystem responses. However, there are a number of assumptions and decisions that go into the OMP analysis that can generate uncertainties in the representation of the mixing and proportions of the source waters. These decisions include the selection of source water regions and definition of water masses, among others. Previous studies (e.g. Thomson and Krassovski, 2010, BO19, Schultz et al., 2024) defined the PEW region located in the eastern tropical North Pacific and transported by the Northern Subsurface Countercurrent (NSCC, Fig. 1). However, new studies (e.g. Margolskee et al., 2019; Gómez-Valdivia et al., 2017) suggest alternate PEW source locations. Our objective is to explore the sensitivity of OMP results to those decisions and assess the capacity of the previous OMP analysis performed in the southern CCS (BO19) to resolve water mass contributions given a more comprehensive understanding of the method's sensitivity to assumptions. We perform several sensitivity analyses using the configuration of the OMP described in BO19 as a baseline and check the stability of the resulting water mass distributions. We focus on PSUW and PEW because of their important association with commercial fish species. Understanding the uncertainties of OMP assumptions will benefit similar studies in other regions, especially in other eastern boundary upwelling systems (EBUS) and other regions characterized by a confluence and mixing of large-scale water masses. Section 2 describes the OMP analysis, assumptions, and rationale behind the sensitivity experiments. Section 3 describes the resulting changes in PSUW and PEW relative contributions in the southern CCS. We discuss these results and their implications in Section 4.

2. Datasets and methods

2.1. Water masses, source water types, and the classical optimum multiparameter (OMP) analysis

The main principle underlying the OMP approach is that the conservative physical and chemical properties of a water sample/parcel are the result of the mixing of a certain number of well-defined water masses, called the source water types (SWT) or end-members present upstream. The distinction between water masses and SWTs is that water masses refers to a volume of water with a common formation history, having its origin in a particular region of the ocean and with physical and chemical properties distinct from its surroundings (Tomczak, 1999a,b). While SWTs is a mathematical definition (a point in a n-dimensional parameter space) that refers to the original properties of a water mass in its formation area without a physical extent (i.e. a volume, see, e.g. Glover et al., 2011; Tomczak, 1999a,b for a more complete discussion). SWTs can be then considered fingerprints of water masses, allowing their labeling and tracking their spreading and mixing processes (Liu and Tanhua, 2021). Here we use the terminology of "water masses", acknowledging that the properties of the water masses used for this analysis actually refer to SWTs.

Once the SWT and their physical and biogeochemical properties are defined, the mixing of the SWT in a water sample and the contribution of each end-member is solved in the OMP using an optimization procedure by minimizing the residuals of a set of linear mixing equations. Mathematically, the OMP finds an optimal solution to a linear system of mixing equations with the contribution of end-members (i.e. SWTs) as variables and the hydrographic properties as the parameters of the system. The classical OMP uses conservative hydrographic properties (Tomczak, 1981), while the extended OMP (eOMP) uses non-conservative properties (Karstensen and Tomczak, 1997; Poole and Tomczak, 1999). Both OMP analyses assume that mass is conserved and the contributions of the different SWTs must be positive. In this manuscript, we utilize the extended OMP (eOMP) package that was developed for the Matlab statistical computing language (source: https://omp.geomar.de/node6.html).

2.2. The extended optimum multiparameter (eOMP) analysis: assumptions and control experiment

In water samples that do not exhibit the characteristics of a single SWT, conservative properties are assumed to be the consequence of the linear mixing of several SWTs. Thus, the first step is to determine/select which predefined SWTs represent the "unmixed" water masses that feed the CCS, and what physical and chemical properties are assumed to remain constant with time in the formation area. In our baseline or control experiment (CTRL hereinafter), we follow the assumptions from BO19. We first define upper and lower end members for each SWT (i.e. upper and lower PSUW, ENPCW, and PEW) by taking the end points of linear segments on θ/S diagrams constructed from the mean temperature and salinity profile (BO19 Fig. 1b and Table S1). This approach, also known as "an archetype analysis" (Cutler and Breiman, 1994), assumed that each SWT is defined by two end-member "subtypes" (i.e. upper and lower SWT), representing a mixture that effectively spans the property values represented by the SWT. The properties that we use to define each SWT are potential temperature (θ), salinity (S), oxygen (O_2), nitrate (NO_3), phosphate (PO_4), and silicic acid (SiO_4), defined in Table 1. Classical OMP resolves the system assuming that all those properties are conservative (i.e. they have no sources or sinks in the ocean interior). However, in our case this assumption was not acceptable as the end-members were defined at the north and tropical Pacific wide scale and thus highly susceptible to organic matter remineralization. We use those hydrographic properties as parameters in the eOMP equation system. With six SWTs and their six properties (i.e. input variables), we are left with a system of six equations plus conservation of mass:

$$
\begin{aligned}
X_{PEWu}T_{PEWu} + \ldots + X_{ENPCWd}T_{ENPCWd} + 0 &= T_{OBS} + R_T \\
X_{PEWu}S_{PEWu} + \ldots + X_{ENPCWd}S_{ENPCWd} + 0 &= S_{OBS} + R_S \\
X_{PEWu}O_{2,PEWu} + \ldots + X_{ENPCWd}O_{2,ENPCWd} - r_{O/P}\Delta P &= O_{2,OBS} + R_{O2} \\
X_{PEWu}PO_{4,PEWu} + \ldots + X_{ENPCWd}PO_{4,ENPCWd} + \Delta P &= PO_{4,OBS} + R_{PO4} \\
X_{PEWu}NO_{3,PEWu} + \ldots + X_{ENPCWd}NO_{3,ENPCWd} + r_{N/P}\Delta P &= NO_{3,OBS} + R_{NO3} \\
X_{PEWu}SiO_{4,PEWu} + \ldots + X_{ENPCWd}SiO_{4,ENPCWd} + r_{Si/P}\Delta P &= SiO_{4,OBS} + R_{SiO4} \\
X_{PEWu} + X_{PEWd} + X_{PSUWu} + X_{PSUWd} + X_{ENPCWu} + X_{ENPCWd} &= 1 + R_{\Sigma}
\end{aligned}
\tag{1}
$$

where *X* is the relative contribution (or mixing fractions) of each SWT, *r* is the Redfield ratios relative to phosphate, *ΔP* is the change in phosphate due to remineralization, *R* is a residual term, and OBS refers to the observed properties from our data. The last equation expresses the condition of mass conservation, which is an additional mixing constraint. Since the system is overestimated, a non-negative least

Table 1
Matrix of mean property values for the upper and lower end members of source water masses: PSUW, ENPCW, and PEW. Data obtained from the World Ocean Database (WOD18).

	$PSUW_{upper}$	$PSUW_{lower}$	$ENPCW_{upper}$	$ENPCW_{lower}$	PEW_{upper}	PEW_{lower}
Sigma-theta (kg m^{-3})	25.6	26.4	25.0	25.8	26.2	26.8
Temperature (°C)	7.75	6.88	18.77	12.89	13.41	9.47
Salinity	32.80	33.69	34.97	34.18	34.85	34.68
Oxygen (mLL^{-1})	6.24	4.58	5.32	4.94	1.06	0.42
Phosphate ($mmolL^{-1}$)	1.16	1.75	0.14	0.66	2.04	2.73
Silicic Acid ($mmolL^{-1}$)	14.81	34.05	3.87	9.85	22.06	39.72
Nitrate ($mmolL^{-1}$)	10.33	22.21	0.25	7.58	28.38	36.41

square technique can be applied to find the solution of the unknown x and *ΔP*. In matrix notation, this linear mixing can be written as:

$$Gx = d + R \tag{2}$$

where G is the SWT matrix, d is the vector containing the observational data that defines our water sample, R is the residual vector, and x is the unknown solution vector (i.e. the relative contribution or mixing fractions). Following Tomczak and Large (1989), the G matrix is normalized and weighted to ensure that the input variables have comparable units and to account for their environmental variability and measurement inaccuracies. We then solve by least square introducing the diagonal weighting matrix W and minimizing the residuals:

$$R^T R = (Gx - d)^T W^T W (Gx - d) \tag{3}$$

where subscripts T denote the transposes of the matrices. The final values of the mixing fractions (x) can be influenced by the weighting of equations, which are determined following Tomczak and Large (1989) as follows:

$$Wj = \sigma_j^2 \Big/ \delta_{jmax} \tag{4}$$

where σ_j^2 is the spatial variance of each property (j) in the SWT matrix G and δ_{jmax} is the largest of the property variances in each source region. In this procedure, the mass balance is treated as if it were a mixing equation. Since there is no measurement involved in this equation, it is not possible to attribute such a weighting factor to the mass balance equation. The usual procedure is then to assign the mass conservation equation with the same weighting as the parameter with the highest weight (Tomczak and Large, 1989; Poole and Tomczak, 1999). For our CTRL experiment (same as in BO19), we use the following weights for each parameter: potential temperature (12), salinity (3), oxygen (7), phosphate (5), silicic acid (2), nitrate (7), and mass (12).

We finally solve this set of equations minimizing the residuals using a least square method constrained to having nonnegative X and ΔP values.

2.3. Sensitivity experiments

As seen in the previous section, there are a number of assumptions and decisions in the eOMP analysis that can generate uncertainties in the representation of the mixing and proportions of the source waters. In this section, we explore alternative decisions to the ones considered in BO19 and quantify the sensitivity of the OMP results to these changes.

2.3.1. Experiment 1: sensitivity to parameter weights

Not all properties are equally reliable for the eOMP. While some properties are difficult to measure, others may have higher spatial and temporal variability (Tomczak and Large, 1989). To account for these differences, all parameters in the eOMP equations are weighted. Although the weighting of the parameters can be performed in a variety of ways, we compute the weights as the ratio of the spatial variance of a given property across the sample domain to the measurement uncertainty for that property in the source water region, following BO19 and Jenkins et al. (2015) (equation (4)). Because the final weights influence the final fractions of the SWTs in the mixing and to account for the uncertainty in the weights, we conduct an experiment using three sets of different weights that focus on changing the weight of Nitrate: low N (N weight = 2), lower N (N weight = 1), and lowest N (N weight = 0.5). In this sensitivity analysis, we mainly focus on changing the weight of the nitrate because it is the macronutrient with the highest weight in BO19 and because its subsurface concentration is highly correlated with primary production in the southern CCS (Jacox et al., 2016; Mantyla et al., 2008). The weights for all the parameters used in the sensitivity analysis are shown in Table 2.

2.3.2. Experiment 2: sensitivity to redfield ratios

A restriction for using the classical OMP analysis is that the analysis needs to be confined to a predefined ocean region (e.g. an oceanic front, intertidal belt), so the mixing of the SWTs can be assumed not to be influenced by biogeochemical processes (i.e. assume all the parameters to be quasi-conservative). However, in our regional-scale analysis for the southern CCS, biogeochemical processes cannot be ignored since the SWTs are defined far away from the water sample (Karstensen and Tomczak, 1997) and their chemical properties (nutrients and oxygen) can be modified by non-conservative processes, such as biological uptake or remineralization. For phosphate, we express the change of phosphate concentration due to biogeochemical processes as an

Table 2
Detailed values of the weights, Redfield ratios and the PEW source regions for the CTRL and Sensitivity eOMP experiments.

		Weights	PEW source region	Redfield ratio (O_2:N:Si)
CTRL BO2019		T10, S3, O10, P5, Si2, N7, M10	10°x 10°box centered at 5°N and 108°W (PEW at NSCCS)	−170:16:18
Weight experiments	Low N	T10, S3, O10, P5, Si2, N2, M10	Same as CTRL	Same as CTRL
	Lower N	T10, S3, O10, P3, Si3, N1, M10	Same as CTRL	Same as CTRL
	Lowest N	T20, S3, O10, P5, Si2, N0.5, M10	Same as CTRL	Same as CTRL
Adjusted Redfield ratio experiment		Same as CTRL	Same as CTRL	−124:13:19
PEW source region experiments	PEW NEUC Jet	Same as CTRL	10°x 10°box centered at 12°N, 108°W	Same as CTRL
	PEW NEUC Jet and MCC	Same as CTRL	3° × 12° box centered at 14°N, 104°W	Same as CTRL
	PEW MCC	Same as CTRL	3° × 5° box centered at 15.5°N, 97.5°W	Same as CTRL
No biogeochemical properties experiment		T10, S3, M10	Same as CTRL	No Redfield ratios used

unknown ΔP quantity. In the other cases, the Δ nutrient is calculated with respect to ΔP using the Redfield ratios as coefficients for conversion between phosphorus and oxygen, nitrogen, and silicon (equation (1)). BO19 established the Redfield ratios on the CTRL experiment as: $r_{-O2/P} = 170$, $r_{N/P} = 16$, and $r_{Si/P} = 18$. The values of $r_{-O2/P}$ and $r_{N/P}$ followed Anderson and Sarmiento (1994) and represent average values with depth in the Pacific Ocean, and the value of $R_{Si/P}$ followed Brzezinski (1985). However, it is important to note that the Redfield ratios are spatiotemporally variable, especially in upwelling regions (Schlesinger, 2013). In this experiment we use alternate Redfield ratios of $r_{-O2/P} = 124$, $r_{N/P} = 13$, and $r_{Si/P} = 19$, which are in good agreement with observed Redfield ratios in the southern CCS (Martz et al., 2014) (Supplementary Fig. S1).

2.3.3. *Experiment 3: sensitivity to the location of the Pacific Equatorial Water source region*

Previous works (BO19; Schultz et al., 2024) defined a PEW source region centered at 5°N and 108°W (red box in Fig. 1), assuming that PEW is transported westward by the Northern Subsurface Countercurrent (NSCC). Using reverse Lagrangian particle tracking, Margolskee et al. (2019) and Gomez-Valdivia et al. (2015) showed that almost 50 % of the subsurface water entering the eastern tropical North Pacific comes from the NSCC, while ~25 % comes from the zonal advection from the North Equatorial Undercurrent Jets (NEUC jets). In addition, along the coast, the subsurface Mexican Coastal Current flows northward and reaches the western coast of Baja California, connecting the tropics with the CU (Gómez-Valdivia et al., 2015), and controlling its semi-annual intensification (Gómez-Valdivia et al., 2017). Based on this main subsurface circulation in the eastern North Pacific (Fig. 1), we investigate the sensitivity of the eOMP results to the change of the source region of PEW. In addition to the region of the NSCC as the main source of the PEW (as in BO19), we also use 3 other regions that include: the NEUC Jet (Jet), the MCC (MCC), and a region that includes both the NEUC Jet and the MCC (JetMCC, Fig. 1 panel b). We keep the weights as in BO19 in all the experiments.

2.3.4. *Experiment 4: sensitivity of the eOMP to the biogeochemical properties*

The physical and biogeochemical properties in the southern CCS have been consistently sampled by the California Cooperative Oceanic Fisheries Investigations (CalCOFI) program since 1984, making this hydrographic data unique not only in the length of the time-series, but also in the variety of hydrographic and biological data. However, other regions are not as well sampled as CalCOFI. In this final sensitivity experiment, we explore the effect of the fractional contributions of the SWT assuming that biogeochemical properties are not sampled or are not available. For this, we use the classical OMP analysis, using only basic hydrographic physical properties: temperature and salinity. Because of the reduction in the number of hydrographic properties (and input parameters), the classical OMP cannot resolve the same 6 SWTs as in the eOMP. We solve this for the lower PSUW and PEW, and upper ENPCW. Values of potential temperature and salinity for this G matrix are the same as given in Table 1.

2.4. *Datasets*

Since 1984, the CalCOFI program has conducted quarterly surveys (usually in January, April, July and October) over six lines in the southern CCS (top right panel in Fig. 1). Stations are designated by a line and station number, with nominal station spacing of approximately 36 km nearshore and 70 km offshore. CalCOFI maintains a bottle database (https://calcofi.org/data/oceanographic-data/bottle-database/) that contains temperature, salinity, nutrient and dissolved oxygen measurements taken from Nisken bottles. Casts are typically to 520 m depth, or until the bottom. In general, bottle samples are taken at 10 m resolution in the upper 100 m and at 20–40 m intervals at larger depths. For the OMP analyses profiles of all variables were linearly interpolated to 5 m intervals. The years extracted from the database covered 1993 to 2018.

SWT were obtained over the regional boxes shown in Fig. 1 by querying the World Ocean Database (https://www.nodc.noaa.gov/OC5/SELECT/dbsearch/dbsearch.html) search criteria set to extract all measured variables in the OSD (Ocean Station Data) dataset. For oxygen and nutrients, a cast was kept for the analysis if it had a simultaneous observation of temperature and salinity. After outlier removal, all casts were averaged together given a single profile for each variable for each water mass location. For each water mass, upper and lower end members were determined by inspecting θ/S diagrams (constructed from the mean temp and salinity profiles) and identifying the end-points of linear segments on the θ/S diagrams. Then all property values at the upper/lower depths were used to construct the G matrix.

3. Results

We focus our results on the two SWTs with largest contributions in the southern CCS: PSUW and PEW, and compare results from the sensitivity runs with those from the CTRL (i.e. BO19). We present these contributions in several ways: (i) maps on isopycnal surfaces representing the upper ($\sigma_\theta = 25.8$ kg/m^3) and lower ($\sigma_\theta = 26.5$ kg/m^3) pycnocline to highlight changes in PSUW and PEW advection along isopycnals (Bograd et al., 2015), respectively; (ii) vertical sections along CalCOFI Lines 80 and 93. Line 80 includes the offshore Station 80.80, typically within the main core of the CC (Lynn and Simpson, 1987); and Line 93 includes Station 93.30, located over the continental slope within the Southern California Bight (SCB) and strongly impacted by the CU (Bograd et al., 2015; Lynn and Simpson, 1987, 1990); and (iii) time series at Stations 80.80 and 93.30.

3.1. *Mean contribution of PSUW on the 25.8 isopycnal surface and along CalCOFI Line 80*

Along the isopycnal 25.8, the mean contribution of PSUW varies with a latitudinal gradient from ~65 % in the offshore regions of Pt. Conception (northern boundary of the CalCOFI domain) to ~58 % in the southern boundary of the CalCOFI domain, reflecting the advection of the CC into the southern CCS. The lowest percentages (~50 %) of PSUW are found along the coast (Fig. 2). Decreasing the weights of the nitrate in the eOMP (i.e. Low N and Lower N experiments) produces a slight decrease (<5 %) in the mean contribution of the PSUW in the offshore regions, and a slight increase (~2 %) along the coast in the SCB, while the representation of the mean contribution of PSUW in the Lowest N experiment is very similar to the CTRL. The modification of the Redfield ratios reduces (~6 %) the magnitude of the mean contribution of PSUW along the coast of the SCB. Changing the location of the PEW source increases the overall contribution of the PSUW along the 25.8 isopycnal in the CalCOFI domain, except in the region of the Channel Islands. While the Jet experiment increases PSUW content by ~5–7 %, the JetMCC and MCC experiments increase PSUW between 10 and 15 % in the overall domain. Excluding the biogeochemical parameters in the eOMP alters the spatial distribution of PSUW, resulting in a greater contribution in the southern boundary compared to the northern boundary, and increasing the PSUW mean contribution up to ~80 % across the domain.

Along Line 80, the offshore area between 100 and 300 m exhibits the highest contribution of PSUW (~65 %), with a smaller contribution from ~60 km to the coast and between 100 and 200 m (Fig. 3). Below 350 m, the elevated PSUW contribution is attributed to the constraints in the eOMP and is not representative of PSUW content at these depths. Changing the weights and Redfield ratios results in a decrease (~10–15 %) in the main contribution of the PSUW between ~170 and 250 m along the northern boundary of the CalCOFI domain. This reduction in the PSUW content extends along all of Line 80 in the Redfield ratio experiment, while in the weights experiment the PSUW content

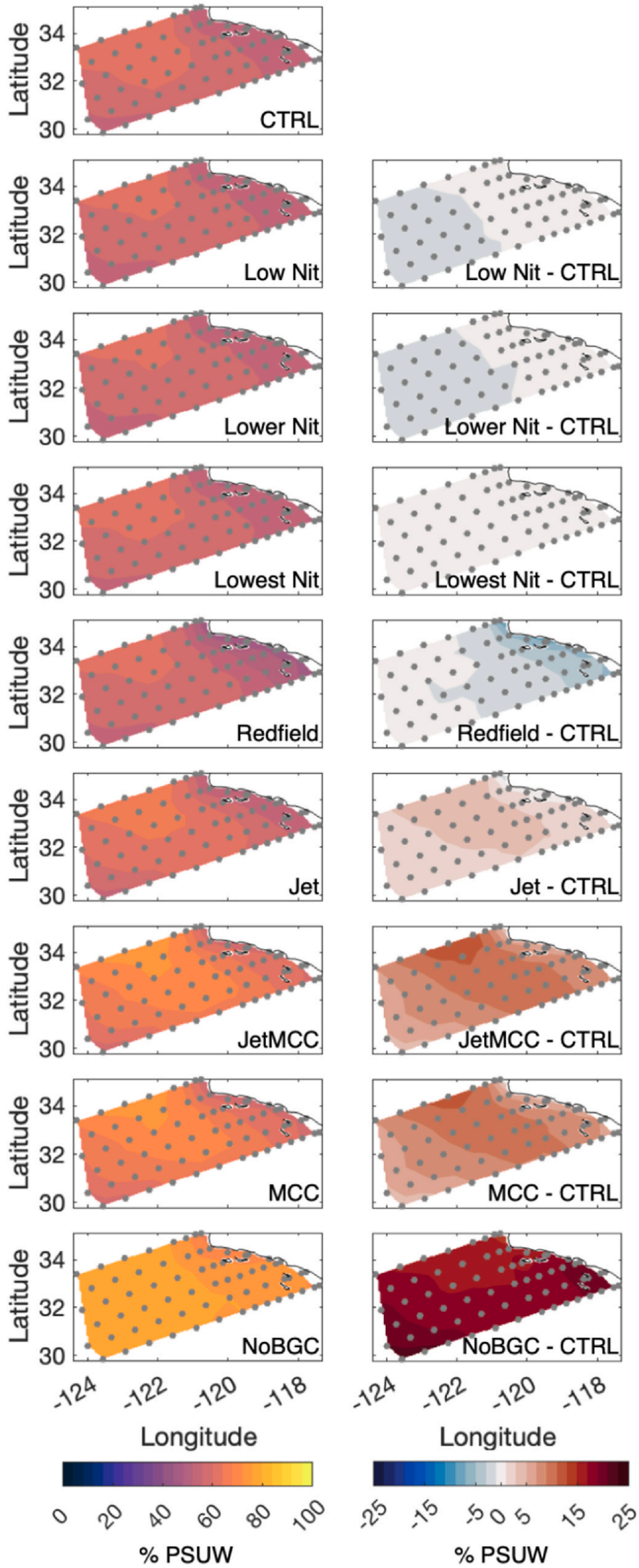

Fig. 2. Maps of the (left) annual mean PSUW content for the CTRL and sensitivity experiments and (right) the difference in %PSUW between the sensitivity experiments and the CTRL on the 25.8 isopycnal surface. Grey dots represent the location of the CalCOFI stations.

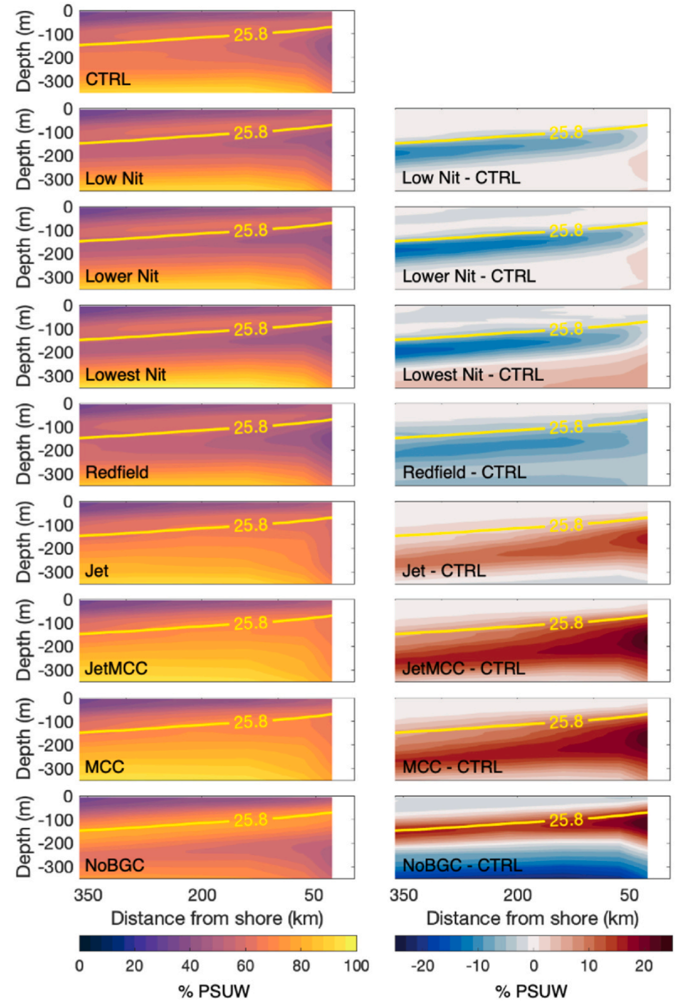

Fig. 3. Vertical sections of the (left) annual mean PSUW content for the CTRL and sensitivity experiments and (right) the difference in %PSUW between the sensitivity experiments and the CTRL along Line 80. Yellow lines represent the 25.8 isopycnal surface. (For interpretation of the references to colour in this figure legend, the reader is referred to the Web version of this article.)

increases slightly (~5 %) primarily near the coast and below ~180 m. The experiments changing the location of the PEW source regions experiments lead to an increase in the vertical PSUW content along Line 80. The JetMCC and MCC experiments result in the highest increases (~20–25 %), extending from the coast to ~150 km below the 25.8 isopycnal. Similarly, the NoBGC experiment produces an increase in the PSUW content between 50 and 150m; however, it produces a decrease in the PSUW content below 200 m.

3.2. Mean contribution of PEW on the 26.5 isopycnal surface and along CalCOFI Line 93

Along the isopycnal 26.5, the mean contribution of PEW exhibits an offshore gradient with its highest contribution (>55 %) along the coast, reflecting the advection of the PEW by the core of the CU (Fig. 4). Changing the weights in the eOMP produces a decrease (~5 %) of the highest PEW contribution along the coast of the SCB. In these Weights experiments, there is almost no change in the offshore regions along the 26.5 isopycnal. The experiments changing the location of the PEW source regions decreases the total PEW content along the 26.5 isopycnal. The JetMCC and MCC experiments lead to a maximum decrease (~15 %) in both the southern coast of the SCB and in the offshore regions. The Jet experiment produces an increase (~5 %) in the PEW content from Pt.

Conception to the Channel Islands. Excluding the biogeochemical parameters in the eOMP slightly decreases the PEW content along the southern coast of the SCB, but increases (~10 %) the PEW content in the offshore regions.

On the southern boundary of the CalCOFI domain, along Line 93, the highest percentage of PEW extends from the coast to 300 km from shore and between 150 and 300 m (Fig. 5). Assigning smaller weights to nitrate slightly affects the PEW contribution on shallower isopycnals. However, when decreasing the nitrate weight and increasing the weights of T, O, and M (Lowest N experiment), the PEW distribution increases/decreases by (~10 %) in shallower/deeper isopycnals than the 26.5. In the Redfield ratio experiment, the vertical distribution of PEW contribution increases (~10 %) from 200 km offshore and between ~150 and 300 m in depth. In contrast, the location of the PEW source region experiments leads to a decrease in the PEW content along Line 93, with up to ~20 % decrease between 100 and 200 m in the JetMCC and MCC experiments. Another important change with these source water region experiments is the offshore extent of maximum %PEW (i.e. reflection of the core of the CU). These three experiments produce a weaker PEW signature farther offshore than the CTRL experiment. Above the isopycnal 26.5, the exclusion of the noBGC experiment also produces a decrease in the PEW content, but the magnitude is larger ~40 % from the coast to ~400 km offshore. Below the 26.5 isopycnal, this experiment increases the PEW content ~15 %.

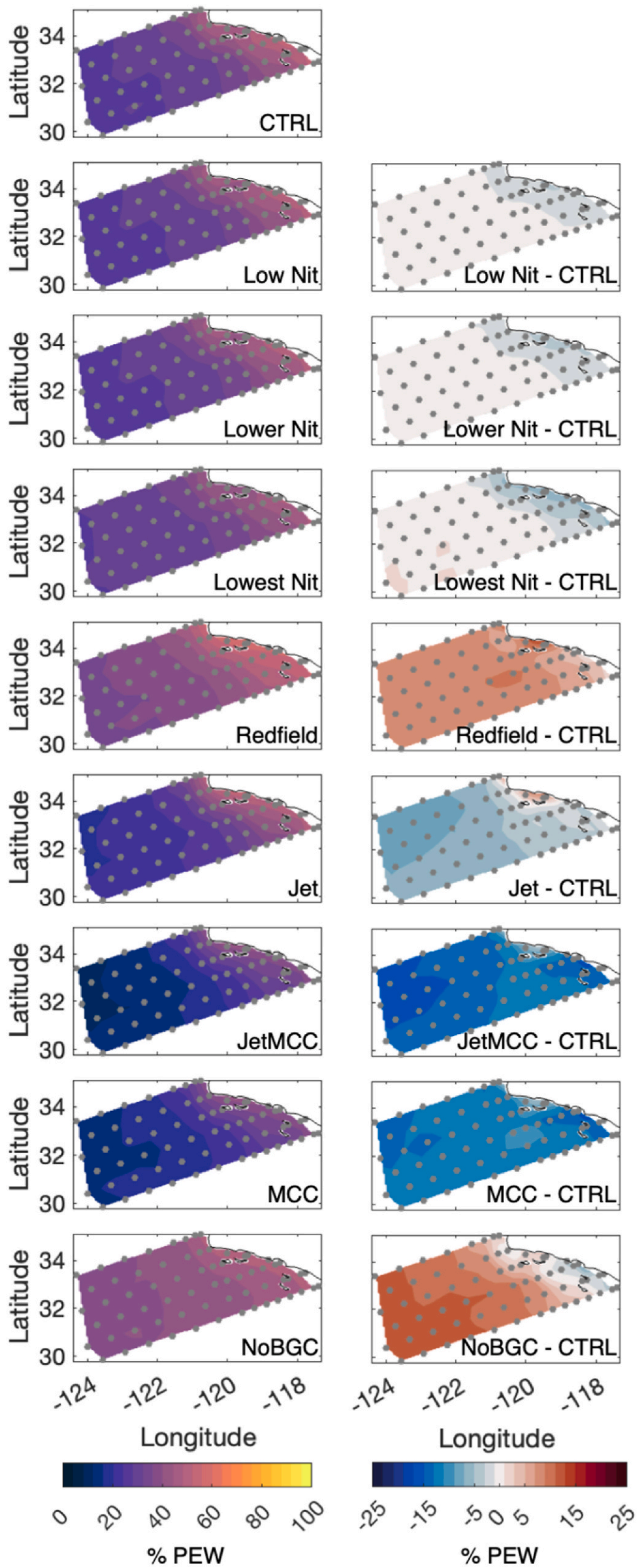

Fig. 4. Maps of the (left) annual mean PEW content for the CTRL and sensitivity experiments and (right) the difference in %PEW between the sensitivity experiments and the CTRL on the 26.5 isopycnal surface. Grey dots represent the location of the CalCOFI stations.

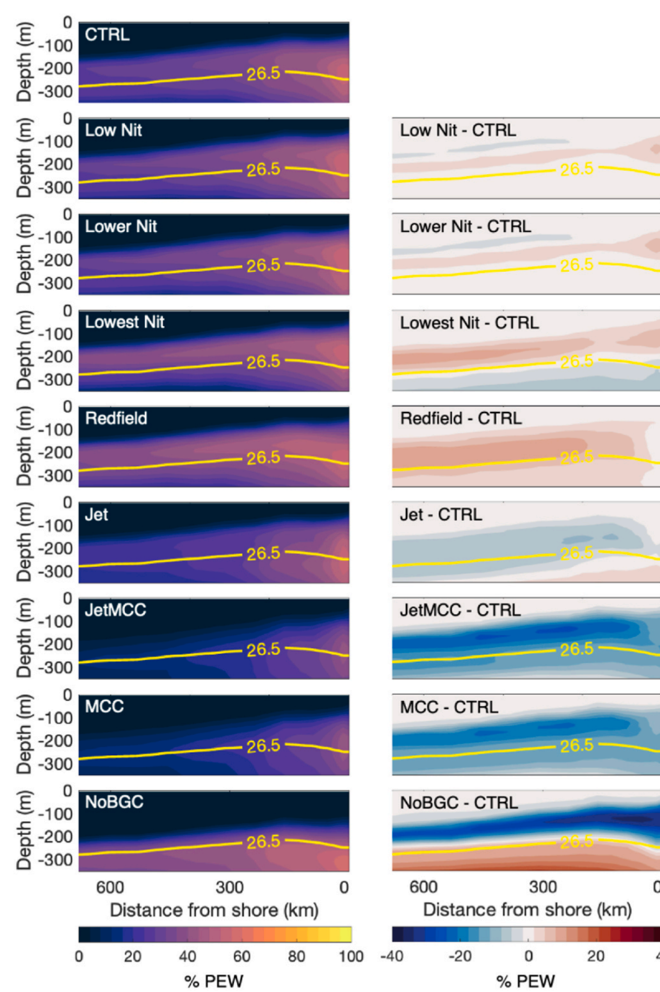

Fig. 5. Vertical sections of the (left) annual mean PEW content for the CTRL and sensitivity experiments and (right) the difference in %PEW between the sensitivity experiments and the CTRL along Line 93. Yellow lines represent the 26.5 isopycnal surface. (For interpretation of the references to colour in this figure legend, the reader is referred to the Web version of this article.)

4. Discussion and conclusions

Tracking variability in the spatial patterns of relative water mass contributions is important to understand changes in ocean circulation and material flux, as well as biogeochemical and ecological processes. Estimated source water contributions to the pycnocline in the southern CCS are sensitive to user assumptions and decisions that go into the eOMP analysis. We have assessed here the eOMP sensitivity to changes in the weighting of the parameters, Redfield ratio, location of the PEW source region, and also limiting the eOMP to only physical parameters (θ,S). Estimated contributions of PSUW and PEW are more sensitive to the location of the PEW source region and the Redfield ratio than to the parameter weights. From the location of the PEW source regions both the JetMCC and MCC experiments have a similar effect on the relative contribution of the water masses, increasing (~25 %) and decreasing (~20 %) the contribution of PSUW and PEW, respectively, in the southern CCS. These effects are most noticeable near the coast, around the core of the CU (150–300 m). The Redfield ratio experiment yields a decrease of PSUW (~15 %) and an increase of PEW (~20 %). Above 250 m, the directions of these changes are similar to the ones from the weights experiment (although the magnitude of the changes is smaller in the latter), suggesting the importance of the relative concentration of nitrate and oxygen in resolving the mixing in the southern CCS. Of all our sensitivity tests, excluding biogeochemical properties from the eOMP changed the contributions of the PSUW and PEW most compared to the CTRL experiment. This result is particularly evident in the spatial pattern of the PEW contribution along Line 93, causing a displacement of the PEW main contribution to deeper isopycnals than the 26.5 surface, which is not consistent with the observed position of the CU (e.g. Thomson and Krassovski, 2010).

The sensitivity experiments conducted here showed that changes in the eOMP configuration predominantly affect the mean magnitude and spatial distribution of the PSUW and PEW contributions, while the temporal variability of the contributions of these water masses remains largely consistent in the sensitivity experiments when compared to the CTRL experiment (Supplementary Fig. S2 and Table S2). Only the PEW source region experiments and the exclusion of the biogeochemistry have an impact on the temporal variability, particularly in the PEW contribution. However, even if these changes in temporal variability are small, these uncertainties on the relative contribution of the source water in the CCS can have an impact on the responses of the ecosystem. For example, greater contributions of PEW bring warmer waters to the region and have been associated with an increase in the richness of warm water species of ichthyoplankton (e.g. McClatchie et al., 2016, 2018). A decrease in the %PEW associated with a change in the location of the PEW could result in less warm-water transported by the CU, and an ichthyoplankton species evenness decline, while its compensated increase in %PSUW could favor the growth and survival of rockfishes in the southern CCS (Schroeder et al., 2019; Fennie et al., 2023). Because water mass contributions and their properties play an important role regulating ecosystem structure and function in the CCS, obtaining accurate representation of these water masses and their variability is key for developing indicators of ecosystem functioning.

These sensitivity analyses can inform other works that focus on more comprehensive analyses of the contributions of the water masses along the entire California Current System using model outputs instead of observations, especially for accounting for the uncertainty and biases in the physical and biogeochemical modeled properties. Since the location of the PEW source regions produces the most dramatic changes in the distribution and contribution of the PEW in the southern CCS, future work will focus on a Lagrangian particle tracking experiment to better constrain the end-members and provide information on water mass pathways.

Based on the results from the set of sensitivity analysis performed here, we recommend that OMP users carefully select which hydrographic properties to use, how to weight the individual constraints, and focus especially on the definition and selection of the characteristics of the SWTs when their source regions are not well known. Future work could benefit from comparisons between different eOMP methods, such as the Matlab package (used here) and the Python-based PYOMPA (Shrikumar et al., 2022). Alternative eOMP implementations may introduce specific differences, such as allowing for a bidirectional (i.e. anaerobic and aerobic) remineralization (Evans et al., 2023) and excluding the mass conservation equation from the SWT matrix. We encourage OMP users to explore and contrast various implementations beyond the Matlab-based approach used here. We highlight here the quality and longevity of programs like CalCOFI that allow reducing uncertainties in our hydrographic samples and deviations from the Redfield ratios, allowing more confident OMP assumptions. Recently, Schultz et al. (2024), applied the OMP analysis to the output of the biogeochemical Argo floats on the CCS, with the constraints of using only temperature, salinity and oxygen. However, longer time series of the source water regions are still required, especially of other biogeochemical properties. Strategic placement of autonomous observation platforms such as Argo floats and gliders, with longer sampling periods and the inclusion of biogeochemical sensors, has potential for resolving large-scale oceanographic drivers of regional processes, especially in EBUS where ecosystems variability is driven not only by local atmospheric forcing but also the large-scale dynamics of oceanic circulation and water masses.

CRediT authorship contribution statement

Mercedes Pozo Buil: Writing – review & editing, Writing – original draft, Visualization, Investigation, Formal analysis, Conceptualization. **Isaac Schroeder:** Writing – review & editing, Investigation, Formal analysis, Conceptualization. **Steven J. Bograd:** Writing – review & editing, Conceptualization. **Michael G. Jacox:** Writing – review & editing, Conceptualization. **Elliott L. Hazen:** Writing – review & editing. **Dianne Deauna:** Writing – review & editing. **Emanuele Di Lorenzo:** Writing – review & editing. **Nicole S. Lovenduski:** Writing – review & editing, Conceptualization. **Samuel Mogen:** Writing – review & editing, Conceptualization. **Ryan R. Rykaczewski:** Writing – review & editing, Conceptualization.

Data availability

All data are open access and freely available. The data for the water types is from the World Ocean Database data and are available at https://www.nodc.noaa.gov/OC5/SELECT/dbsearch/dbsearch.html. Observational bottle data for the OMP is from CalCOFI and are available at https://calcofi.org/data/oceanographic-data/bottle-database/. Information on conducting an OMP analysis and sample code are available using the Matlab OMP toolbox, https://www.mathworks.com/matlabcentral/fileexchange/1334-omp-analysis.

Declaration of competing interest

The authors declare that they have no known competing financial interests or personal relationships that could have appeared to influence the work reported in this paper.

Acknowledgments

This work was supported by the funding from the National Oceanic and Atmospheric Administration Climate Variability and Predictability Program (NA20OAR4310405 and NA24OARX431C0020), and the Modeling, Analysis, Predictions and Projections Program (NA20OAR4310447). We acknowledge the quality and longevity of the CalCOFI program, and the many scientists and seagoing staff who have contributed to the collection, processing, and analysis of this excellent data set. We thank Eric Bjorkstedt for helpful comments on an earlier

version of the manuscript.

Appendix A. Supplementary data

Supplementary data to this article can be found online at https://doi.org/10.1016/j.dsr2.2025.105498.

Data availability

Data will be made available on request.

References

Anderson, L.A., Sarmiento, J.L., 1994. Redfield ratios of remineralization determined by nutrient data analysis. Global Biogeochemical Cycles 8 (1), 65–80. https://doi.org/10.1029/93GB03318.

Bograd, S.J., Pozo Buil, M., Lorenzo, E.D., Castro, C.G., Schroeder, I.D., Goericke, R., Anderson, C.R., Benitez-Nelson, C., Whitney, F.A., 2015. Changes in source waters to the southern California Bight. Ann. Rev. Mar. Sci 15. https://doi.org/10.1016/j.dsr2.2014.04.009, 303-328112, 42-52.

Bograd, S.J., Lynn, R.J., 2003. Long-term variability in the southern California current system. Deep-Sea Res. Pt. II: Top. Stud. Oceanogr. 50 (14), 2355–2370. https://doi.org/10.1016/S0967-0645(03)00131-0.

Bograd, S.J., Schroeder, I.D., Jacox, M.G., 2019. A water mass history of the Southern California current system. Geophys. Res. Lett. 46 (12), 6690–6698. https://doi.org/10.1029/2019gl082685.

Brzezinski, M.A., 1985. The Si:C:N ratio of marine diatoms: interspecific variability and the effect of some environmental variables. J. Phycol. 21 (3), 347–357. https://doi.org/10.1111/j.0022-3646.1985.00347.x.

Cutler, A., Breiman, L., 1994. Archetypal analysis. Tech 36 (4), 338–347. https://doi.org/10.2307/1269949.

Evans, N., Schroeder, I.D., Pozo Buil, M., Jacox, M.G., Bograd, S.J., 2020. Drivers of Subsurface Deoxygenation in the Southern California Current System. Geophysical Research Letters 47 (21), e2020GL089274. https://doi.org/10.1029/2020GL089274.

Evans, N., Tichota, J., Moffett, J.W., Devol, A.H., 2023. Prolific nitrite reoxidation across the eastern tropical North Pacific ocean. Limnol. Oceanogr. 68, 1719–1733. https://doi.org/10.1002/lno.12380.

Fennie, H.W., Grorud-Colvert, K., Sponaugle, S., 2023. Larval rockfish growth and survival in response to anomalous ocean conditions. Sci. Rep. 13 (1). https://doi.org/10.1038/s41598-023-30726-5.

García-Ibáñez, M.I., Pérez, F.F., Lherminier, P., Zunino, P., Mercier, H., Tréguer, P., 2018. Water mass distributions and transports for the 2014 GEOVIDE cruise in the North Atlantic. BG. 15 (7), 2075–2090. https://doi.org/10.5194/bg-15-2075-2018.

Glover, D.M., Jenkins, W.J., Doney, S.C., 2011. Modeling Methods for Marine Science. Cambridge University Press. https://doi.org/10.1017/CBO9780511975721.

Gómez-Valdivia, F., Parés-Sierra, A., Flores-Morales, A.L., 2015. The Mexican Coastal Current: a subsurface seasonal bridge that connects the tropical and subtropical Northeastern Pacific. Con. Shelf Res. 110, 100–107. https://doi.org/10.1016/j.csr.2015.10.010.

Gómez-Valdivia, F., Parés-Sierra, A., Laura Flores-Morales, A., 2017. Semiannual variability of the California undercurrent along the southern California current system: a tropical generated phenomenon. J. Geophys. Res. Oceans 122 (2), 1574–1589. https://doi.org/10.1002/2016jc012350.

Helland-Hansen, B., 1916. Nogen hydrografiske metoder. Forh Skand Naturf Mote 16, 357–359.

Jacox, M.G., Hazen, E.L., Bograd, S.J., 2016. Optimal environmental conditions and anomalous ecosystem responses: constraining bottom-up controls of phytoplankton biomass in the California current system. Sci. Rep. 6 (1), 27612. https://doi.org/10.1038/srep27612.

Jenkins, W.J., Smethie, W.M., Boyle, E.A., Cutter, G.A., 2015. Water mass analysis for the U.S. GEOTRACES (GA03) North Atlantic sections. Deep-Sea Res. Pt. II: Top. Stud. Oceanogr. 116, 6–20. https://doi.org/10.1016/j.dsr2.2014.11.018.

Karstensen, J., Tomczak, M., 1997. Ventilation processes and water mass ages in the thermocline of the southeast Indian Ocean. Geophys. Res. Lett. 24 (22), 2777–2780. https://doi.org/10.1029/97gl02708.

Liu, M., Tanhua, T., 2021. Water masses in the Atlantic Ocean: characteristics and distributions. Ocean Sci. 17 (2), 463–486. https://doi.org/10.5194/os-17-463-2021.

Llanillo, P.J., Karstensen, J., Pelegrí, J.L., Stramma, L., 2013. Physical and biogeochemical forcing of oxygen and nitrate changes during El Niño/El Viejo and La Niña/La Vieja upper-ocean phases in the tropical eastern South Pacific along 86° W. BG. 10 (10), 6339–6355. https://doi.org/10.5194/bg-10-6339-2013.

Lynn, R.J., Simpson, J.J., 1987. The California Current system: the seasonal variability of its physical characteristics. J. Geophys. Res. 92 (C12), 12947. https://doi.org/10.1029/jc092ic12p12947.

Lynn, R.J., Simpson, J.J., 1990. The flow of the undercurrent over the continental borderland off southern California. J. Geophys. Res. Oceans 95 (C8), 12995–13008. https://doi.org/10.1029/jc095ic08p12995.

Mackas, D.L., Denman, K.L., Bennett, A.F., 1987. Least squares multiple tracer analysis of water mass composition. J. Geophys. Res. Oceans 92 (C3), 2907–2918. https://doi.org/10.1029/jc092ic03p02907.

Mantyla, A.W., Bograd, S.J., Venrick, E.L., 2008. Patterns and controls of chlorophyll-a and primary productivity cycles in the Southern California Bight. J. Mar. Syst. 73 (1), 48–60. https://doi.org/10.1016/j.jmarsys.2007.08.001.

Margolskee, A., Frenzel, H., Emerson, S., Deutsch, C., 2019. Ventilation pathways for the North pacific oxygen deficient zone. Glob. Biogeochem. Cycles 33 (7), 875–890. https://doi.org/10.1029/2018gb006149.

Martz, T., Send, U., Ohman, M.D., Takeshita, Y., Bresnahan, P., Kim, H.-J., Nam, S., 2014. Dynamic variability of biogeochemical ratios in the southern California current system. Geophys. Res. Lett. 41 (7), 2496–2501. https://doi.org/10.1002/2014gl059332.

McClatchie, S., Gao, J., Drenkard, E.J., Thompson, A.R., Watson, W., Ciannelli, L., Bograd, S.J., Thorson, J.T., 2018. Interannual and secular variability of larvae of Mesopelagic and forage fishes in the southern California current system. J. Geophys. Res.: Oceans (San Franc.) 123 (9), 6277–6295. https://doi.org/10.1029/2018jc014011.

McClatchie, S., Thompson, A.R., Alin, S.R., Siedlecki, S., Watson, W., Bograd, S.J., 2016. The influence of pacific equatorial water on fish diversity in the southern California current system. J. Geophys. Res. Oceans 121 (8), 6121–6136. https://doi.org/10.1002/2016jc011672.

Montgomery, R.B., 1958. Water characteristics of Atlantic Ocean and of world ocean. Deep-Sea Res. 5 (2), 134–148. https://doi.org/10.1016/0146-6313(58)90004-2.

Pardo, P.C., Pérez, F.F., Velo, A., Gilcoto, M., 2012. Water masses distribution in the Southern Ocean: improvement of an extended OMP (eOMP) analysis. Prog. Oceanogr. 103, 92–105. https://doi.org/10.1016/j.pocean.2012.06.002.

Poole, R., Tomczak, M., 1999. Optimum multiparameter analysis of the water mass structure in the Atlantic Ocean thermocline. Deep-Sea Res. I: Ocean. Res. Papers 46 (11), 1895–1921. https://doi.org/10.1016/S0967-0637(99)00025-4.

Schlesinger, W. H. Bernhardt, 2013. Biogeochemistry: an Analysis of Global Change.

Schroeder, I.D., Santora, J.A., Bograd, S.J., Hazen, E.L., Sakuma, K.M., Moore, A.M., Edwards, C.A., Wells, B.K., Field, J.C., 2019. Source water variability as a driver of rockfish recruitment in the California Current Ecosystem: implications for climate change and fisheries management. Can. J. Fish. Aquat. Sci. 76 (6), 950–960. https://doi.org/10.1139/cjfas-2017-0480.

Schultz, C., Dunne, J.P., Liu, X., Drenkard, E., Carter, B., 2024. Characterizing subsurface oxygen variability in the California current system (CCS) and its links to water mass distribution. J. Geophys. Res. Oceans 129 (2). https://doi.org/10.1029/2023jc020000.

Shrikumar, A., Lawrence, R., Casciotti, K.L., 2022. Pyompa technical note. https://doi.org/10.1002/essoar.10507053.4.

Thomson, R.E., Krassovski, M.V., 2010. Poleward reach of the California Undercurrent extension. J. Geophys. Res. 115 (C9). https://doi.org/10.1029/2010jc006280.

Tomczak, M., 1981. A multi-parameter extension of temperature/salinity diagram techniques for the analysis of non-isopycnal mixing. Prog. Oceanogr. 10 (3), 147–171. https://doi.org/10.1016/0079-6611(81)90010-0.

Tomczak, M., 1999a. Some historical, theoretical and applied aspects of quantitative water mass analysis. J. Mar. Res. 57 (2), 275–303. https://doi.org/10.1357/002224099321618227.

Tomczak, M., 1999b. Potential vorticity as a tracer in quantitative water mass analysis. Matthias Tomczak. International WOCE Newsletter, Number 36, 6–10. ISSN 1029-1725 September 1999.

Tomczak, M., Large, D.G.B., 1989. Optimum multiparameter analysis of mixing in the thermocline of the eastern Indian Ocean. J. Geophys. Res. Oceans 94 (C11), 16141–16149. https://doi.org/10.1029/jc094ic11p16141.

You, Y., Tomczak, M., 1993. Thermocline circulation and ventilation in the Indian Ocean derived from water mass analysis. Deep-Sea Res. I: Oceanogr Res. Papers 40 (1), 13–56. https://doi.org/10.1016/0967-0637(93)90052-5.